The Journal of Chemical Physics

RESEARCH ARTICLE | JULY 01 2026

Green–Kubo relation in a mesoscale odd fluid model

Special Collection: Statistical Physics: From Quantum Fluctuations to Soft Matter and Viral Assemblies

Yujing Ouyang ; Yuxing Jiao ; Fangfu Ye ; Mingcheng Yang

J. Chem. Phys. 165, 014901 (2026)
https://doi.org/10.1063/5.0336634

The Journal of Chemical Physics | ARTICLE | pubs.aip.org/aip/jcp

Green–Kubo relation in a mesoscale odd fluid model

Cite as: J. Chem. Phys. 165, 014901 (2026); doi: 10.1063/5.0336634
Submitted: 1 April 2026 • Accepted: 10 June 2026 •
Published Online: 1 July 2026

Yujing Ouyang,[1,2] Yuxing Jiao,[1,2] Fangfu Ye,[1,2,a)] and Mingcheng Yang[1,2,a)]

AFFILIATIONS

[1] Beijing National Laboratory for Condensed Matter Physics and Laboratory of Soft Matter Physics, Institute of Physics, Chinese Academy of Sciences, Beijing 100190, China
[2] School of Physical Sciences, University of Chinese Academy of Sciences, Beijing 100049, China

Note: This paper is part of the Special Topic on Statistical Physics: From Quantum Fluctuations to Soft Matter and Viral Assemblies.
[a)] **Authors to whom correspondence should be addressed:** fye@iphy.ac.cn and mcyang@iphy.ac.cn

ABSTRACT

Fluids, characterized by broken time-reversal and parity symmetries, exhibit odd transport phenomena where longitudinal drivings can induce transverse fluxes. Recently, a mesoscale model called chiral stochastic rotation dynamics (CSRD) has been developed to simulate odd fluids with high computational efficiency. In this work, we verify the Green–Kubo relations for both normal and odd transport coefficients in this model, confirming that this model correctly captures the underlying statistical relationship between macroscopic transport and microscopic fluctuations in odd fluids. This work solidifies the physical foundation of the CSRD model, paving the way for its application in studying the statistical physics and nonequilibrium behavior of odd fluids.

I. INTRODUCTION

Certain fluid systems exhibit anomalous transport phenomena where a thermodynamic force can drive a nondissipative flux in the perpendicular direction. Such fluids are known as odd fluids, and such transport phenomena are referred to as odd transport, including odd diffusion,[1–3] odd viscosity,[4–9] and odd thermal conductivity.[10–12] Odd transport behavior is characterized by a nonvanishing antisymmetric part in the transport coefficient tensor, which is deeply rooted in the microscopic dynamics of odd fluids that break time-reversal and parity symmetries.[12–15] It has been shown that the Green–Kubo relations, which connect the transport coefficients to the spontaneous flux fluctuations in steady state,[16–19] may still be valid for odd fluids.[3,9,20,21] These relations are critical for understanding the physical mechanisms that govern the transport behavior of odd fluids.

However, large-scale simulation of odd fluids, especially odd complex fluids, presents significant computational challenges because of their many-body nature and intricate interactions. Existing molecular-dynamics-based models for odd fluids[3,9,22–26] suffer from considerable computational bottlenecks. Conversely, highly efficient coarse-grained methods[27–37] have been primarily developed for the conventional complex fluids and lack the mechanisms to capture odd transport phenomena. To bridge this gap, our recent work[38] introduced a coarse-grained model named chiral stochastic rotation dynamics (chiral SRD or CSRD). Built upon the conventional SRD framework, the CSRD model maintains its advantages such as high computational efficiency, proper hydrodynamics, and thermal fluctuations, while uniquely reproducing significant odd diffusion, odd viscosity, and odd thermal conductivity.

Although the CSRD model properly reproduces three important odd transport behaviors, it is not *a priori* guaranteed that all the other underlying physics are also correctly captured due to the model's coarse-graining nature. Clearly, an excellent coarse-grained fluid model should capture real fluid physics as much as possible. This motivates us to verify the Green–Kubo relations in this model to confirm its thermodynamic reliability and self-consistency, as has been achieved for the conventional SRD model.[39–42] In addition, regarding direct numerical verification, while the Green–Kubo relations for odd diffusion and odd viscosity have been verified in some specific active odd fluid models,[3,9,21] the relation for odd thermal conductivity has, to the best of our knowledge, not been confirmed in any odd fluid. The CSRD model would thus provide a unique platform to address this gap and complete the picture.

In this paper, we systematically investigate the Green–Kubo relations for both normal and odd transport coefficients in the CSRD fluid. By comparing the transport coefficients obtained from equilibrium flux correlation functions and from independent nonequilibrium measurements, we verify these relations for diffusion, viscosity, and thermal conductivity. This work solidifies the physical foundation of the CSRD model, confirming its broad potential for investigating the statistical physics and nonequilibrium behavior of odd fluids.

This paper is organized as follows. In Sec. II, we recall the basic description of the CSRD model. In Secs. III–V, we, respectively, verify the Green–Kubo relations for diffusion coefficient, viscosity, and thermal conductivity in the CSRD fluid. In Sec. VI, we analyze the time reversal symmetry breaking in the CSRD fluid at the level of correlation functions within the Green–Kubo relations. Furthermore, in Sec. VII, we apply the CSRD approach to validate the Einstein relation for an immersed colloidal particle.

II. THE CSRD MODEL

The CSRD model is based on the SRD model but features unique chirality. For simplicity, we restrict our discussion to two dimensions.

The conventional SRD model is composed of a large number of point-like particles moving in continuous space, experiencing alternating streaming and collision steps. In the streaming step, the position $\boldsymbol{r}_i(t)$ of each particle (denoted by i) is updated ballistically during a fixed discretized time step Δt,

$$\boldsymbol{r}_i(t+\Delta t) = \boldsymbol{r}_i(t) + \boldsymbol{v}_i(t)\Delta t, \tag{1}$$

with $\boldsymbol{v}_i(t)$ being the velocity of the ith particle, which will then be updated in the subsequent collision step. To perform a coarse-grained collision, the particles are divided into a meshgrid of square cells and exchange velocities only with particles in the same cell. The position of the meshgrid is randomly shifted before every collision step to ensure the Galilean invariance.[43] In the collision step, the velocity $\boldsymbol{v}_i(t)$ is updated as follows:

$$\boldsymbol{v}_i(t+\Delta t) = \boldsymbol{v}_{cm}(t) + \boldsymbol{R}(\Omega)\cdot(\boldsymbol{v}_i(t) - \boldsymbol{v}_{cm}(t)), \tag{2}$$

which means the velocities of each particle relative to the center-of-mass velocity $\boldsymbol{v}_{cm}(t)$ in each cell are rotated by an angle Ω. For each cell in each collision step, Ω is independently and randomly chosen as ω or $-\omega$ with equal probability.

In our CSRD model, an extra rotational angle θ is added into the collision step Eq. (2) to introduce chirality. Now, for each cell in each collision step, Ω is independently and randomly chosen as $\omega+\theta$ or $-\omega+\theta$ with equal probability. θ effectively introduces a nonzero average rotation angle, which breaks the time-reversal and parity symmetries of the collision process and, in turn, enables the emergence of odd transport coefficients. Reversing the sign of θ corresponds to a parity transformation by flipping the average net rotation, which will map the odd transport coefficients to their negatives and leave the normal coefficients unchanged. θ is called the chiral angle of the CSRD model. When $\theta = 0$, the CSRD model reduces to the SRD model, which is nonchiral. Like the SRD model, the CSRD model locally conserves mass, momentum, and energy and has an equilibrium steady state.[38]

We point out that, although the chirality can be alternatively implemented by setting Ω to be $\pm\omega$ with unequal probabilities, the current method is more straightforward and easier to generalize to three dimensions.[44] While the nonzero rotational angle θ is reminiscent of the effect of the external magnetic fields on charged particle systems, they are essentially different. In the latter, chirality is encoded in the single-particle trajectories that are continuously deflected by the Lorentz force, and the interactions between particles are symmetric and nonchiral.[45–47] In contrast, in the CSRD model, the streaming step is force-free and nonchiral. Chirality enters exclusively through the collision step, which is a multi-particle interaction process not reducible to a single-particle effect. Both mechanisms can give rise to odd transport phenomena at the macroscopic level.

Below, we perform simulations to test the Green–Kubo relations for this two dimensional mesoscale CSRD fluid. The simulation parameters are set as follows unless otherwise specified: mean temperature $k_BT = 1$, $\Delta t = 0.1$, particle mass $m = 1$, cell size $a = 1$, mean particle number density $n = 10$, and random rotational angle $\omega = 2\pi/3$.

III. DIFFUSION COEFFICIENT

The constitutive relation of diffusion reads

$$J_\alpha = -D_{\alpha\beta}\partial_\beta C, \tag{3}$$

where the diffusive flux J_α is related to the concentration gradient $\partial_\beta C$ through the diffusivity tensor $D_{\alpha\beta}$. In a two-dimensional isotropic fluid, $D_{\alpha\beta}$ takes the form

$$D_{\alpha\beta} = D\delta_{\alpha\beta} + D_o\varepsilon_{\alpha\beta}, \tag{4}$$

with $\delta_{\alpha\beta}$ being the symmetric Kronecker delta and $\varepsilon_{\alpha\beta}$ being the antisymmetric Levi–Cività tensor. Here, D is the normal self-diffusion coefficient that drives the flux parallel to the gradient, while D_o is the odd self-diffusion coefficient that drives the flux perpendicular to the gradient.[3]

The general form of the Green–Kubo relation for the diffusivity tensor is in integral,

$$D_{\alpha\beta} = \int_0^\infty dt\big\langle v_\alpha(t)v_\beta(0)\big\rangle. \tag{5}$$

However, in the context of the CSRD model, where the time step is discretized, the Green–Kubo relation takes the form[39]

$$D_{\alpha\beta} = \Delta t\left(\frac{1}{2}\big\langle v_\alpha(0)v_\beta(0)\big\rangle + \sum_{n=1}^{\infty}\big\langle v_\alpha(n\Delta t)v_\beta(0)\big\rangle\right), \tag{6}$$

with v_α being the velocity component of a diffusing CSRD particle. Figure 1 shows the Green–Kubo measurement of D and D_o using Eqs. (4) and (6). As expected, D and D_o are, respectively, the even and odd functions of θ, as the sign of θ controls the chiral rotation direction.

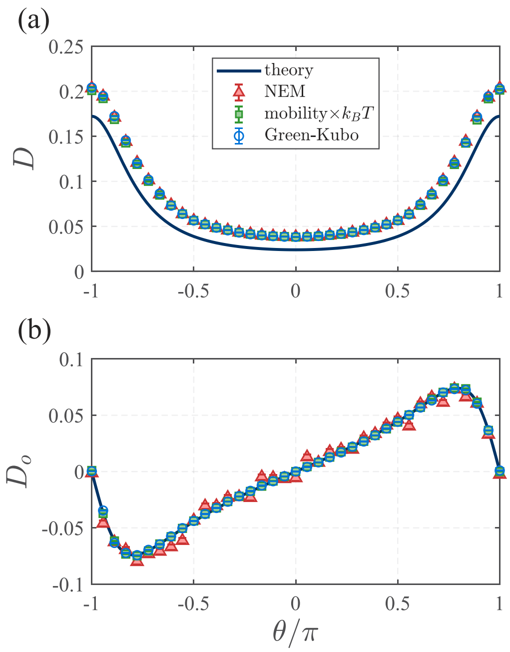

FIG. 1. (a) Normal diffusion coefficient D and (b) odd diffusion coefficient D_o measured for different chiral rotational angles θ. Blue circles are results measured by the Green–Kubo relation. Red triangles are results obtained by the nonequilibrium measurement (NEM). Green squares are the results of mobility multiplied by k_BT. Solid lines are the theoretical predictions of D and D_o (which are derived under the molecular chaos approximation and can deviate from the simulation results. See Ref. 38). Green–Kubo integrals are calculated up to $600\Delta t$ to ensure convergence. External force is set along the y-axis, i.e., $\boldsymbol{F}^{ex} = F_y^{ex}\mathbf{e}_y$, with $F_y^{ex} = -1$. Simulation box size is $L_x \times L_y$, with $L_x = L_y = 20$ for the Green–Kubo and mobility measurement, and $L_x = 20, L_y = 40$ for the NEM simulation.

For comparison, we determine D and D_o independently by using the nonequilibrium scheme. We apply a boundary-driven concentration gradient to the CSRD fluid and measure the diffusive particle fluxes parallel and perpendicular to the gradient direction. We then quantify D and D_o using Eqs. (3) and (4) (Details of this method are described in Ref. 38). As demonstrated in Fig. 1, the results obtained from the nonequilibrium method are consistent with those measured by the Green–Kubo relation, thus verifying the Green–Kubo relation for diffusion coefficients of the mesoscale odd fluid.

Furthermore, we measure the mobility aiming to verify the Einstein relation in the CSRD fluid. In simulations, the mobility is measured by driving a tagged fluid particle with a constant external force $\boldsymbol{F}^{ex}$. The remaining fluid particles are each applied with an inverse force $-\boldsymbol{F}^{ex}/(N-1)$ to guarantee that the total external force on the system is zero (N being the particle number). Under the external force, the streaming step [Eq. (1)] is modified as follows:

$$\begin{aligned} \boldsymbol{r}_i(t+\Delta t) &= \boldsymbol{r}_i(t) + \boldsymbol{v}_i(t)\Delta t + \frac{\boldsymbol{F}_i}{2m}\Delta t^2, \\ \boldsymbol{v}_i^s(t) &= \boldsymbol{v}_i(t) + \frac{\boldsymbol{F}_i}{m}\Delta t, \end{aligned} \tag{7}$$

where the superscript s indicates the velocity after the streaming step. The collision step is then based on $\boldsymbol{v}_i^s(t)$,

$$\boldsymbol{v}_i(t+\Delta t) = \boldsymbol{v}_{cm}^s(t) + \boldsymbol{R}(\Omega)\cdot(\boldsymbol{v}_i^s(t) - \boldsymbol{v}_{cm}^s(t)). \tag{8}$$

We apply the simple scaling thermostat to keep the system temperature constant. After the system reaches the steady state, the terminal velocity $\boldsymbol{U}$ of the tagged particle is measured. The constitutive relation between $\boldsymbol{F}^{ex}$ and $\boldsymbol{U}$ is given by

$$U_\alpha = \mu_{\alpha\beta}F_\beta^{ex}, \tag{9}$$

where the mobility tensor takes the form

$$\mu_{\alpha\beta} = \mu\delta_{\alpha\beta} + \mu_o\varepsilon_{\alpha\beta}. \tag{10}$$

Here, μ is the normal mobility and μ_o is the odd mobility,[47,48] which are calculated using Eqs. (9) and (10). As shown in Fig. 1, the values of $k_BT\mu$ and $k_BT\mu_o$ coincide with D and D_o, respectively, confirming the validity of the Einstein relation in the CSRD fluid (see the Appendix for an approximate theoretical proof).

IV. VISCOSITY

The constitutive relation of viscosity reads

$$\sigma_{\alpha\beta}^{vis} = \eta_{\alpha\beta\mu\nu}\dot{e}_{\mu\nu}, \tag{11}$$

where the viscous stress tensor $\sigma_{\alpha\beta}^{vis}$ is related to the velocity gradient tensor $\dot{e}_{\mu\nu} = \partial_\nu v_\mu$ through the viscosity tensor $\eta_{\alpha\beta\mu\nu}$. In a two-dimensional isotropic fluid, the viscosity tensor $\eta_{\alpha\beta\mu\nu}$ can be expressed as the linear combination of six distinct viscosities η, ζ, η_R, η_o, η_A, η_B,

$$\begin{aligned} \eta_{\alpha\beta\mu\nu} = {}& \eta\left(\delta_{\alpha\mu}\delta_{\beta\nu} + \delta_{\alpha\nu}\delta_{\beta\mu} - \delta_{\alpha\beta}\delta_{\mu\nu}\right) + \zeta\delta_{\alpha\beta}\delta_{\mu\nu} + \eta_R\left(\delta_{\alpha\mu}\delta_{\beta\nu} - \delta_{\alpha\nu}\delta_{\beta\mu}\right) \\ & + \eta_o\left(\varepsilon_{\alpha\mu}\delta_{\beta\nu} + \varepsilon_{\beta\nu}\delta_{\alpha\mu}\right) - \eta_A\varepsilon_{\alpha\beta}\delta_{\mu\nu} - \eta_B\delta_{\alpha\beta}\varepsilon_{\mu\nu}. \end{aligned} \tag{12}$$

Here, η represents the shear viscosity, ζ the bulk viscosity, η_R the rotation–rotation viscosity, η_o the odd viscosity, η_A the compression–rotation viscosity, and η_B the rotation–compression viscosity. The physical interpretations of these viscosities are detailed in Ref. 9.

The general form of the Green–Kubo relation for the viscosity tensor is given by

$$\eta_{\alpha\beta\mu\nu} = \frac{A}{k_BT}\int_0^\infty dt\left\langle\hat{\sigma}_{\alpha\beta}^{vis}(t)\hat{\sigma}_{\mu\nu}^{vis}(0)\right\rangle. \tag{13}$$

Similar to the case of diffusivity, in the CSRD model, the Green–Kubo integral should be expressed as a summation over correlation terms,

$$\eta_{\alpha\beta\mu\nu} = \frac{A\Delta t}{k_BT}\left(\frac{1}{2}\left\langle\hat{\sigma}_{\alpha\beta}^{vis}(0)\hat{\sigma}_{\mu\nu}^{vis}(0)\right\rangle + \sum_{n=1}^{\infty}\left\langle\hat{\sigma}_{\alpha\beta}^{vis}(n\Delta t)\hat{\sigma}_{\mu\nu}^{vis}(0)\right\rangle\right), \tag{14}$$

where A is the area of the system. According to Refs. 41 and 42, the *instantaneous* stress tensor in the CSRD system is given by

$$\hat{\sigma}_{\alpha\beta}(t) = -\frac{1}{A\Delta t}\sum_j mv_{j\alpha}(t)\left[\xi_{j\beta}^s(t+\Delta t) - \xi_{j\beta}^s(t)\right]. \tag{15}$$

The summation runs over all particles. For particle j, $\boldsymbol{v}_j$ is its velocity and $\boldsymbol{\xi}_j^s$ denotes its cell coordinate in the random-shift frame [e.g., if particle j is located in cell (m, n) with cell size a, then $\boldsymbol{\xi}_j^s = (ma, na)$]. The *instantaneous* viscous stress tensor $\hat{\sigma}_{\alpha\beta}^{vis}$ can be determined using Eq. (15) and the relation $\hat{\sigma}_{\alpha\beta}^{vis} = \hat{\sigma}_{\alpha\beta} + p\delta_{\alpha\beta}$, where $p = nk_BT$ is the hydrostatic pressure of the system. To measure the viscosities using the Green–Kubo relation, we first calculate $\eta_{\alpha\beta\mu\nu}$ through Eqs. (14) and (15), and then use Eq. (12) to extract η, ζ, η_R, η_o, η_A, and η_B. The results are shown in Fig. 2. As expected, η, ζ, and η_R are the even functions of θ, while η_o, η_A, and η_B are the odd ones.

For comparison, we also apply the nonequilibrium method to measure the viscosities independently. We first determine $\eta_{\alpha\beta\mu\nu}$ according to Eq. (11), and then combine them to extract the six distinct viscosities. In simulations, to measure $\eta_{\alpha\beta xy}$, a boundary-driven shear flow is imposed to generate the velocity gradient $\dot{e}_{xy}$, while the other three velocity gradients $\dot{e}_{xx}$, $\dot{e}_{yx}$, and $\dot{e}_{yy}$ remain zero. The stress components $\sigma_{\alpha\beta}$ are measured by computing the momentum fluxes across imaginary planes, and then the constitutive relation Eq. (11) is used to determine $\eta_{\alpha\beta xy}$. (Details of this method can be found in Ref. 38.) $\eta_{\alpha\beta yx}$ are determined in a similar way. To measure $\eta_{\alpha\beta yy}$, a Lees–Edwards-like boundary condition[19] is applied to generate the velocity gradient $\dot{e}_{yy}$, while the other three velocity gradients $\dot{e}_{xx}$, $\dot{e}_{xy}$, and $\dot{e}_{yx}$ remain zero. To be specific, the y-boundary of the system is continuously moved to expand the system slowly,

$$L_y(t + \Delta t) = (1 + \alpha\Delta t)L_y(t), \tag{16}$$

where L_y denotes the system size in the y-direction and α is the constant expanding rate. If the ith particle moves out of the bottom$(-)$ or the top$(+)$ of the simulation box, its position $\boldsymbol{r}_i(t)$ and velocity $\boldsymbol{v}_i(t)$ are replaced by $\boldsymbol{r}_i^{\pm}(t)$ and $\boldsymbol{v}_i^{\pm}(t)$,

$$\begin{aligned}\boldsymbol{r}_i^{\pm}(t) &= \boldsymbol{r}_i(t) \mp L_y(t)\boldsymbol{e}_y,\\ \boldsymbol{v}_i^{\pm}(t) &= \boldsymbol{v}_i(t) \mp \alpha L_y(t)\boldsymbol{e}_y.\end{aligned} \tag{17}$$

The target system size and temperature are the same as those used in the previous Green–Kubo measurement, but the initial temperature should be set higher since the expansion process is adiabatic $(TV = const)$. The stress components $\sigma_{\alpha\beta}$ are measured when the system reaches the target size and temperature. Then, the constitutive relation Eq. (11) is used to solve $\eta_{\alpha\beta yy}$. $\eta_{\alpha\beta xx}$ are determined in a similar way. In this manner, we have successfully measured η, η_R, η_o, η_A, and η_B. However, for the bulk viscosity ζ in the expanding system, we find it difficult to precisely determine the viscous stress σ_{xx}^{vis} and σ_{yy}^{vis}. This is because the hydrostatic pressure p is typically three orders of magnitude larger than σ_{xx}^{vis} and σ_{yy}^{vis}, making it numerically challenging to calculate σ_{xx}^{vis} and σ_{yy}^{vis} precisely. So we adopted an indirect approach to determine ζ. In our previous work,[38] we have theoretically proved that the kinetic part of ζ is zero, while the collisional part of ζ is equal to the collisional part of η. Given that $\eta_{yyyy} = \zeta + \eta$ [derived from Eq. (12)], ζ should be equal to half of the collisional part of η_{yyyy}, which can be measured directly. [The collisional part of viscosity is obtained by substituting the collisional part of the stress into the constitutive relation Eq. (11). The method for measuring the collisional part of the stress is described in Ref. 38.] The results of all six viscosities measured by the nonequilibrium method (see Fig. 2) and by the Green–Kubo relation agree

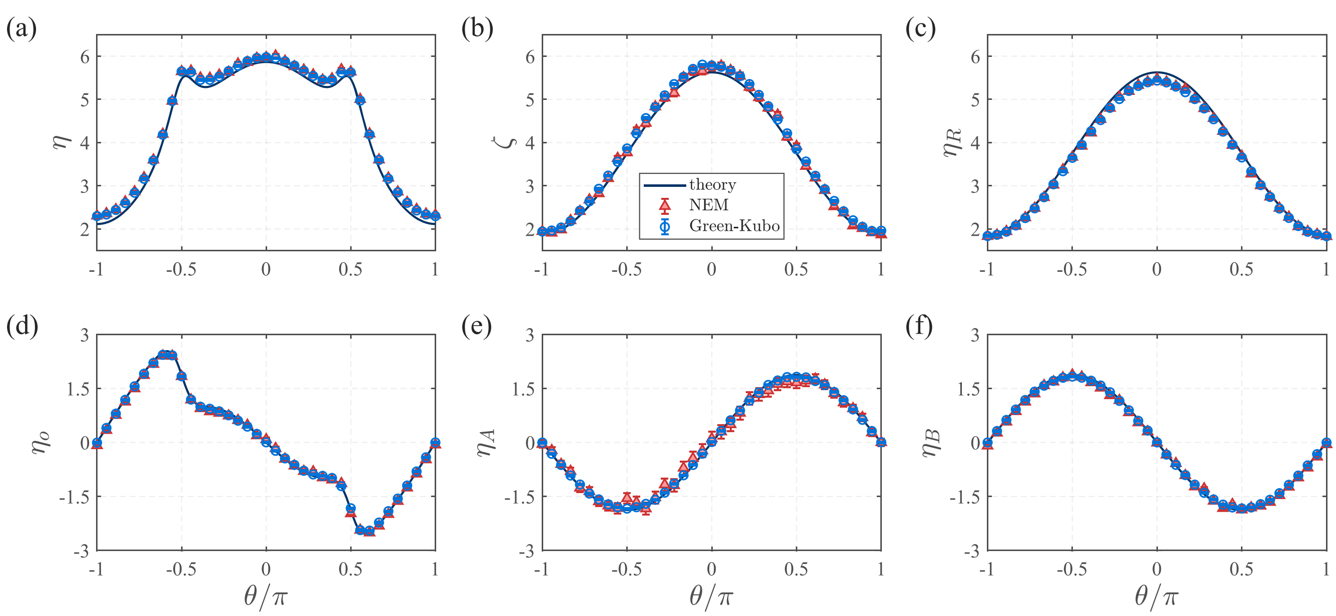

FIG. 2. Viscosities of the CSRD fluid measured for different chiral rotational angles θ. Blue circles are results measured by the Green–Kubo relation. Red triangles are results obtained by the nonequilibrium measurement (NEM). Solid lines are the theoretical predictions of the viscosities (see Ref. 38). Green–Kubo integrals are calculated up to $100\Delta t$ to ensure convergence. Simulation box size $L_x \times L_y = 20 \times 20$ for the Green–Kubo measurement and the shearing NEM. In the expanding NEM, $L_x = 20$, while L_y expands from 19 to 21, with the expanding rate $\alpha = 0.0015$. Measurements take place at $19.95 < L_y < 20.05$.

with each other, thereby corroborating the Green–Kubo relation for viscosities.

V. THERMAL CONDUCTIVITY

The constitutive relation of heat conduction reads

$$J_\alpha^E = -\kappa_{\alpha\beta}\partial_\beta T, \tag{18}$$

where the energy flux J_α^E is related to the temperature gradient $\partial_\beta T$ through the thermal conductivity tensor $\kappa_{\alpha\beta}$. In a two-dimensional isotropic fluid, the thermal conductivity tensor $\kappa_{\alpha\beta}$ takes the form

$$\kappa_{\alpha\beta} = \kappa\delta_{\alpha\beta} + \kappa_o\varepsilon_{\alpha\beta}. \tag{19}$$

Here, κ is the normal thermal conductivity that drives the flux parallel to the gradient, while κ_o is the odd thermal conductivity that drives the flux perpendicular to the gradient.

The general form of the Green–Kubo relation for the thermal conductivity tensor is given by

$$\kappa_{\alpha\beta} = \frac{A}{k_B T^2}\int_0^\infty dt \left\langle \hat{J}_\alpha^E(t)\hat{J}_\beta^E(0)\right\rangle, \tag{20}$$

whose summing form in the CSRD model is

$$\kappa_{\alpha\beta} = \frac{A\Delta t}{k_B T^2}\left(\frac{1}{2}\left\langle \hat{J}_\alpha^E(0)\hat{J}_\beta^E(0)\right\rangle + \sum_{n=1}^{\infty}\left\langle \hat{J}_\alpha^E(n\Delta t)\hat{J}_\beta^E(0)\right\rangle\right). \tag{21}$$

According to Ref. 42, the *instantaneous* energy flux employed in Eq. (21) takes the form

$$\hat{J}_\alpha^E(t) = \frac{1}{A\Delta t}\sum_j \tilde{E}_j(t)\left[\xi_{j\alpha}^s(t+\Delta t) - \xi_{j\alpha}^s(t)\right], \tag{22}$$

with $\tilde{E}_j(t) = \frac{1}{2}mv_j^2(t) - k_B T$. To measure κ and κ_o via the Green–Kubo relation, we first calculate $\kappa_{\alpha\beta}$ through Eqs. (21) and (22), and then use Eq. (19) to extract κ and κ_o. The results are presented in Fig. 3. As expected, κ and κ_o are, respectively, the even and odd functions of θ.

For comparison, we also employ the nonequilibrium simulation method to measure κ and κ_o in the CSRD fluid. Analogous to the case of diffusion coefficient, a boundary-driven temperature gradient is applied to the CSRD fluid, and the corresponding energy flux is measured. Then, κ and κ_o are obtained through Eqs. (18) and (19) (see Ref. 38 for details of this method.). As displayed in Fig. 3, the results obtained from the nonequilibrium measurement agree with those determined by the Green–Kubo relation, which validates the Green–Kubo relation for thermal conductivity in the CSRD fluid.

VI. CORRELATION FUNCTIONS

To see how the introduction of the chiral angle θ leads to nonvanishing odd transport coefficients in the CSRD fluid, we examine the correlation functions in the Green–Kubo relations for some of these coefficients. The odd diffusion coefficient D_o, odd viscosity η_o, and odd thermal conductivity κ_o have their contributing correlation functions denoted by $C_{D_o}(t)$, $C_{\eta_o}(t)$, and $C_{\kappa_o}(t)$, respectively, which can be read from their Green–Kubo relations,

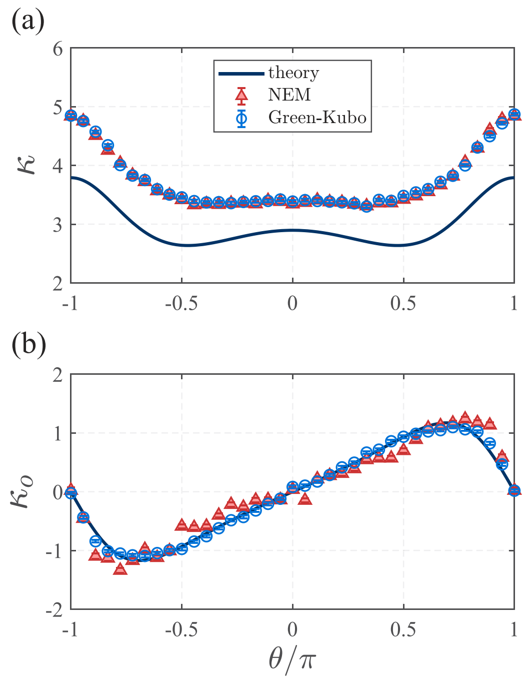

FIG. 3. (a) Normal thermal conductivity κ and (b) odd thermal conductivity κ_o measured for different chiral rotational angles θ. Blue circles are results measured by the Green–Kubo relation. Red triangles are results obtained by the nonequilibrium measurement (NEM). Solid lines are the theoretical predictions of κ and κ_o (which are also derived under the molecular chaos approximation. See Ref. 38). Green–Kubo integrals are calculated up to $100\Delta t$ to ensure convergence. Simulation box size $L_x \times L_y = 20 \times 20$ for the Green–Kubo measurement and the NEM simulation.

$$\begin{aligned} C_{D_o}(t) &= \langle v_x(t)v_y(0)\rangle, \\ C_{\eta_o}(t) &= \left(\left\langle \hat{\sigma}_{xx}^{vis}(t)\hat{\sigma}_{xy}^{vis}(0)\right\rangle - \left\langle \hat{\sigma}_{yy}^{vis}(t)\hat{\sigma}_{xy}^{vis}(0)\right\rangle\right)/2, \\ C_{\kappa_o}(t) &= \left\langle \hat{J}_x^E(t)\hat{J}_y^E(0)\right\rangle. \end{aligned} \tag{23}$$

The time reversal operation is defined as follows:

$$C_{D_o}(t) \to C_{D_o}(-t) = \langle v_x(-t)v_y(0)\rangle = \langle v_x(0)v_y(t)\rangle, \tag{24}$$

where the last equality holds due to time translation invariance in the steady state. Similarly, the other two correlation functions under time reversal are

$$\begin{aligned} C_{\eta_o}(-t) &= \left(\left\langle \hat{\sigma}_{xx}^{vis}(0)\hat{\sigma}_{xy}^{vis}(t)\right\rangle - \left\langle \hat{\sigma}_{yy}^{vis}(0)\hat{\sigma}_{xy}^{vis}(t)\right\rangle\right)/2, \\ C_{\kappa_o}(-t) &= \left\langle \hat{J}_x^E(0)\hat{J}_y^E(t)\right\rangle. \end{aligned} \tag{25}$$

As shown in Fig. 4, when the chiral angle θ is zero and the CSRD fluid reduces to the nonchiral SRD fluid, the correlation functions $C_{D_o}(t)$, $C_{\eta_o}(t)$, and $C_{\kappa_o}(t)$ vanish, resulting in the disappearance of the odd transport coefficients. In contrast, when θ is nonzero, the correlation functions are not vanishing and change sign under time reversal, i.e., $C_{D_o}(t) = -C_{D_o}(-t)$, $C_{\eta_o}(t) = -C_{\eta_o}(-t)$, and

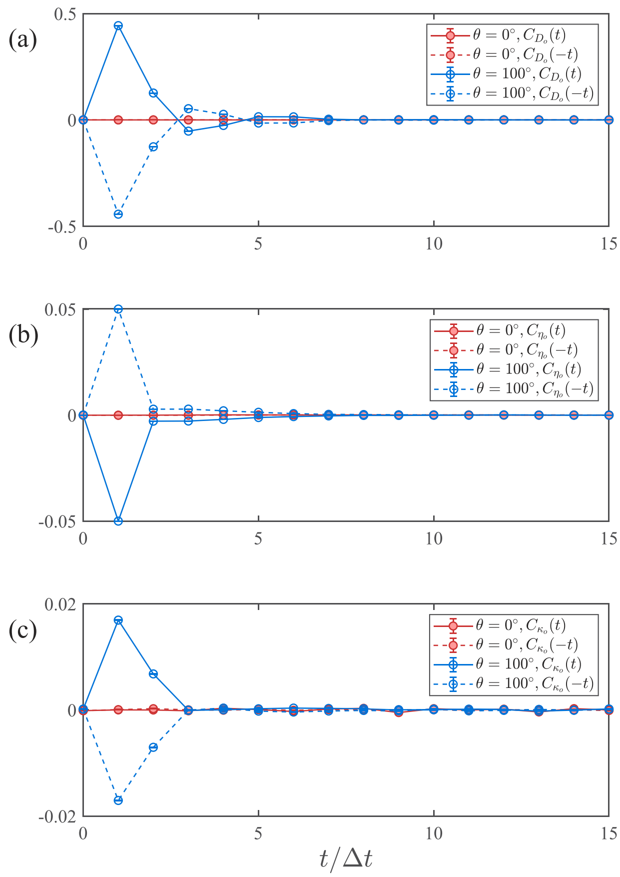

FIG. 4. Correlation functions contributing to (a) odd diffusion coefficient, (b) odd viscosity, and (c) odd thermal conductivity. Simulation box size $L_x \times L_y = 20 \times 20$.

$C_{\kappa_o}(t) = -C_{\kappa_o}(-t)$. These nonvanishing correlation functions finally sum up by the Green–Kubo relations to yield the nonzero odd transport coefficients D_o, η_o, and κ_o.

VII. EINSTEIN RELATION FOR COLLOIDAL PARTICLE

In Secs. III–V, we have studied the Green–Kubo relations in the pure CSRD solvent. In this section, we extend the application of the CSRD model to a colloidal solution and explore whether the Einstein relation holds for a diffusing colloidal particle immersed in the CSRD fluid. To this end, we perform the CSRD-MD hybrid simulation scheme,[34] where the motion of the colloidal particle and the interactions between the colloidal particle and the CSRD particles are simulated by the MD method.

In our simulations, the interaction between the colloidal particle and the CSRD particles is the Weeks–Chandler–Andersen (WCA) potential,

$$U(r) = 4\epsilon\left[\left(\frac{\sigma}{r}\right)^{12} - \left(\frac{\sigma}{r}\right)^{6} + \frac{1}{4}\right], \quad r \leqslant 2^{1/6}\sigma, \tag{26}$$

with ϵ being the energy scale and σ the colloid-fluid collision diameter. The mass of the colloidal particle is set as $M_c = mn\pi\sigma^2$. The corresponding equations of motion for the CSRD and colloidal particles are solved by the velocity Verlet algorithm with time step Δt_{MD} during the streaming step. To keep the temperature fixed, we apply the Maxwell–Boltzmann scaling thermostat[49] in the simulations. The simulation parameters for this colloidal solution are the same as those specified in Sec. II except for $\omega = 5\pi/6$, with $\Delta t_{MD} = 0.002$, $\epsilon = 2.5$, and $\sigma = 4$.

The diffusion tensor of the colloidal particle $D^c_{\alpha\beta}$ is measured by the Green–Kubo relation,

$$D^c_{\alpha\beta} = \int_0^\infty dt\langle v^c_\alpha(t) v^c_\beta(0)\rangle, \tag{27}$$

where v^c_α is the velocity component of the colloidal particle. $D^c_{\alpha\beta}$ can be expressed as

$$D^c_{\alpha\beta} = D^c\delta_{\alpha\beta} + D^c_o\varepsilon_{\alpha\beta}, \tag{28}$$

where D^c is the normal diffusivity and D^c_o is the odd diffusivity of the colloidal particle. On the other hand, the mobility tensor of the colloidal particle is measured by driving it via an external force $\boldsymbol{F}^{ex}$. We denote the terminal velocity for the colloidal particle by $\boldsymbol{U}^c$, which can be given by

$$U^c_\alpha = \mu^c_{\alpha\beta}F^{ex}_\beta. \tag{29}$$

The mobility tensor $\mu^c_{\alpha\beta}$ reads

$$\mu^c_{\alpha\beta} = \mu^c\delta_{\alpha\beta} + \mu^c_o\varepsilon_{\alpha\beta}, \tag{30}$$

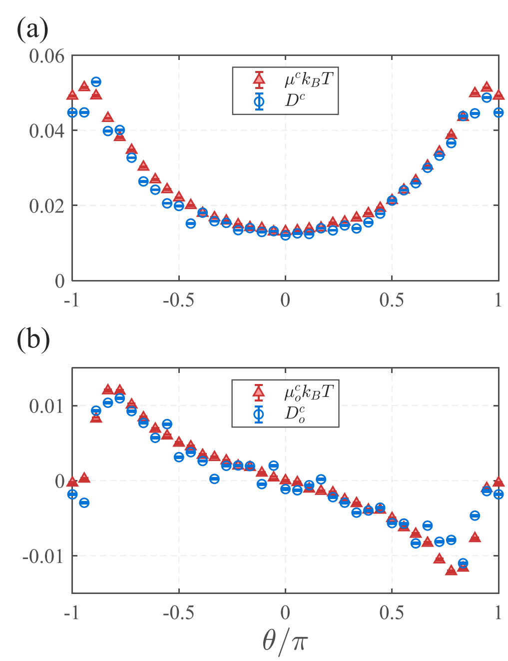

FIG. 5. The verification of the Einstein relation of the colloidal particle. Green–Kubo integrals are calculated up to $2500\Delta t$ to ensure convergence. In the mobility measurement, the external force is set along the y-axis, i.e., $\boldsymbol{F}^{ex} = F^{ex}_y\mathbf{e}_y$, with $F^{ex}_y = 2$. Simulation box size $L_x \times L_y = 80 \times 80$.

with μ^c and μ_o^c the normal and odd mobility of the colloidal particle, respectively. The result shows that the Einstein relation is valid for the colloidal particle diffusing in the CSRD fluid (see Fig. 5).

Interestingly, this application reveals that even a spherically symmetric object can exhibit odd mobility when immersed in an odd fluid. The key factor underlying this phenomenon is the odd viscosity η_o. When a spherical object travels longitudinally through an odd viscous fluid, a symmetric local shear flow field will be created around the object. As a result, the odd viscosity will lead to an asymmetric stress distribution around the object, which in turn generates a net transverse force on the object,[25] giving it an odd mobility.

VIII. DISCUSSION AND CONCLUSION

In this article, we systematically investigate the Green–Kubo relations in the CSRD odd fluid. For all the normal and odd transport coefficients characterizing diffusion, viscosity, and thermal conductivity, we show excellent agreement between the simulation results from the Green–Kubo and nonequilibrium methods. We note that the simulations are performed with a finite system size, which may introduce some deviations to the transport coefficients from their true values in the thermodynamic limit. However, since both the Green–Kubo and nonequilibrium measurements are performed in systems of the same size, the finite-size effect would not affect the consistency between the two methods. Thereby, we validate the Green–Kubo relations for the CSRD fluid. Furthermore, we use the CSRD model to simulate odd complex fluids and verify the Einstein relation for a suspended colloidal particle. These findings solidify the physical foundation of the CSRD model, proving it to be a powerful tool for further research on the statistical physics and nonequilibrium behavior of odd fluids.

ACKNOWLEDGMENTS

This work was supported by the National Key R&D Program of China (Grant No. 2022YFF0503504) and the National Natural Science Foundation of China (Grant Nos. 12274448 and T2325027).

AUTHOR DECLARATIONS

Conflict of Interest

The authors have no conflicts to disclose.

Author Contributions

Yujing Ouyang and Yuxing Jiao contributed equally to this work.

Yujing Ouyang: Conceptualization (equal); Formal analysis (equal); Investigation (equal); Software (equal); Validation (equal); Visualization (equal); Writing – original draft (equal). **Yuxing Jiao**: Conceptualization (equal); Formal analysis (equal); Investigation (equal); Software (equal); Validation (equal); Visualization (equal); Writing – original draft (equal). **Fangfu Ye**: Conceptualization (equal); Formal analysis (equal); Methodology (equal); Project administration (equal); Supervision (equal); Validation (equal); Writing – review & editing (equal). **Mingcheng Yang**: Conceptualization (equal); Formal analysis (equal); Methodology (equal); Project administration (equal); Supervision (equal); Validation (equal); Writing – review & editing (equal).

DATA AVAILABILITY

The data that support the findings of this study are available from the corresponding author upon reasonable request.

APPENDIX: PROOF FOR THE EINSTEIN RELATION IN THE CSRD

In the main text, we have verified the Einstein relation for the CSRD fluid through direct numerical simulations. This Appendix will serve as a complementary display that this relation can be simply derived via an approximate theoretical approach. In the following, we derive the self-diffusion tensor $\boldsymbol{D}$ and the mobility tensor $\boldsymbol{\mu}$ separately to show that the Einstein relation $\boldsymbol{D} = k_B T\boldsymbol{\mu}$ holds in the CSRD.

To begin with, we focus on the motion of a single CSRD particle and write down its equation of motion. The position and velocity at time $t = n\Delta t$ of the particle we selected are denoted by $\boldsymbol{r}(t) \triangleq \boldsymbol{r}_n$ and $\boldsymbol{v}(t) \triangleq \boldsymbol{v}_n$, respectively. Newton's equations of motion for this particle are solved in the streaming step. In the absence of external forces, the particle moves like a free particle,

$$\boldsymbol{r}_n = \boldsymbol{r}_{n-1} + \boldsymbol{v}_{n-1}\Delta t. \tag{A1}$$

In the collision step, this particle is sorted into a collision cell and its velocity in the center-of-mass reference frame of the cell is randomly rotated,

$$\boldsymbol{v}_n = \boldsymbol{v}_{n-1,cm} + \boldsymbol{R}_{n-1}\cdot(\boldsymbol{v}_{n-1} - \boldsymbol{v}_{n-1,cm}), \tag{A2}$$

where $\boldsymbol{v}_{n,cm}$ is the center-of-mass velocity of the cell. For brevity, we introduce the mean velocity of other particles in the cell $\hat{\boldsymbol{v}}_{n-1}$ to rewrite $\boldsymbol{v}_{n-1,cm}$ as

$$\boldsymbol{v}_{n-1,cm} = \frac{1}{N_{n-1,c}}\boldsymbol{v}_{n-1} + \frac{N_{n-1,c}-1}{N_{n-1,c}}\hat{\boldsymbol{v}}_{n-1}, \tag{A3}$$

with $N_{n,c}$ denoting the particle number of the collision cell. Then, Eq. (A2) becomes

$$\boldsymbol{v}_n = \boldsymbol{T}_{n-1}\cdot\boldsymbol{v}_{n-1} + \boldsymbol{L}_{n-1}\cdot\hat{\boldsymbol{v}}_{n-1}, \tag{A4}$$

where $\boldsymbol{T}_n = \boldsymbol{I} - \boldsymbol{L}_n$, $\boldsymbol{I}$ is the unit tensor, and $\boldsymbol{L}_n = (\boldsymbol{I} - \boldsymbol{R}_n)(N_{n,c} - 1)/N_{n,c}$.

The self-diffusion tensor can be derived from the Green–Kubo relation Eq. (6),

$$\boldsymbol{D} = \Delta t \sum_{n=0}^{+\infty}{}' \langle \boldsymbol{v}_n \boldsymbol{v}_0\rangle, \tag{A5}$$

where the prime on the summation symbol indicates that the first term is multiplied by 1/2. According to Eq. (A4), terms in the summation of Eq. (A5) can be calculated as

$$\begin{aligned}\langle \boldsymbol{v}_n \boldsymbol{v}_0 \rangle &= \langle \boldsymbol{T}_{n-1} \cdot \boldsymbol{T}_{n-2} \cdot \dots \cdot \boldsymbol{T}_0 \cdot \boldsymbol{v}_0 \boldsymbol{v}_0 \rangle \\ &= \langle \boldsymbol{T} \rangle^n \cdot \langle \boldsymbol{v}_0 \boldsymbol{v}_0 \rangle \\ &= \langle \boldsymbol{T} \rangle^n \cdot \frac{k_B T}{m} \boldsymbol{I} \\ &= \frac{k_B T}{m} \langle \boldsymbol{T} \rangle^n, \end{aligned} \tag{A6}$$

Here, in the first equality, we apply the molecular chaos assumption, i.e., $\langle \hat{\boldsymbol{v}}_n \boldsymbol{v}_0 \rangle = \boldsymbol{0}$. In the second equality, we assume that the rotations $\boldsymbol{R}_n$ and cell particle numbers $N_{n,c}$ at different times are independently and identically distributed, so $\langle \boldsymbol{T}_n \rangle$ for any n is identical, which is denoted by $\langle \boldsymbol{T} \rangle$. (Similarly, we define $\langle \boldsymbol{L} \rangle = \boldsymbol{I} - \langle \boldsymbol{T} \rangle$.) Substituting $\langle \boldsymbol{v}_n \boldsymbol{v}_0 \rangle$ into the summation (A5), we obtain

$$\begin{aligned}\boldsymbol{D} &= \Delta t \sum_{n=0}^{+\infty} \langle \boldsymbol{v}_n \boldsymbol{v}_0 \rangle - \frac{\Delta t}{2} \langle \boldsymbol{v}_0 \boldsymbol{v}_0 \rangle \\ &= \frac{k_B T \Delta t}{2m} \left(2 \sum_{n=0}^{+\infty} \langle \boldsymbol{T} \rangle^n - \boldsymbol{I} \right) \\ &= \frac{k_B T \Delta t}{2m} \left[2 (\boldsymbol{I} - \langle \boldsymbol{T} \rangle)^{-1} - \boldsymbol{I} \right], \end{aligned} \tag{A7}$$

namely,

$$\boldsymbol{D} = \frac{k_B T \Delta t}{2m} \left(2 \langle \boldsymbol{L} \rangle^{-1} - \boldsymbol{I} \right). \tag{A8}$$

To calculate the mobility tensor of the CSRD particle, we impose an external force $\boldsymbol{F}$ on the selected particle. We assume $\boldsymbol{F}$ is sufficiently small so that the selected particle can be regarded as moving in an isothermal bath. In the steady state, the driving force is balanced by the friction, and the particle moves with a terminal velocity $\boldsymbol{v}_f = (\langle \boldsymbol{r}_n \rangle - \langle \boldsymbol{r}_{n-1} \rangle)/\Delta t$. The mobility tensor $\boldsymbol{\mu}$ is defined by $\boldsymbol{v}_f = \boldsymbol{\mu} \cdot \boldsymbol{F}$. In the following, we look for the relation between $\boldsymbol{v}_f$ and $\boldsymbol{F}$ and derive the mobility tensor. In the presence of the driving force, the streaming step of the selected particle becomes

$$\begin{aligned}\boldsymbol{r}_n &= \boldsymbol{r}_{n-1} + \boldsymbol{v}_{n-1} \Delta t + \frac{\boldsymbol{F}}{2m} \Delta t^2, \\ \boldsymbol{v}_{n-1}^s &= \boldsymbol{v}_{n-1} + \frac{\boldsymbol{F}}{m} \Delta t, \end{aligned} \tag{A9}$$

where the superscript s of $\boldsymbol{v}_{n-1}^s$ means the velocity after the streaming step. Similar to Eq. (A4), the collision step now reads

$$\boldsymbol{v}_n = \boldsymbol{T}_{n-1} \cdot \boldsymbol{v}_{n-1}^s + \boldsymbol{L}_{n-1} \cdot \hat{\boldsymbol{v}}_{n-1}^s. \tag{A10}$$

Using Eqs. (A9) and (A10), the average $\langle \boldsymbol{v}_n \rangle$ is derived as follows:

$$\begin{aligned}\langle \boldsymbol{v}_n \rangle &= \left\langle \boldsymbol{T}_{n-1} \cdot \boldsymbol{v}_{n-1}^s + \boldsymbol{L}_{n-1} \cdot \hat{\boldsymbol{v}}_{n-1}^s \right\rangle \\ &= \langle \boldsymbol{T} \rangle \cdot \left\langle \boldsymbol{v}_{n-1}^s \right\rangle \\ &= \langle \boldsymbol{T} \rangle \cdot \left\langle \boldsymbol{v}_{n-1} + \frac{\boldsymbol{F}}{m} \Delta t \right\rangle. \end{aligned} \tag{A11}$$

In the first equality, we assume the mean background flow velocity remains zero under the small driving force, so that $\langle \hat{\boldsymbol{v}}_{n-1}^s \rangle = \boldsymbol{0}$. In the steady state, we have $\langle \boldsymbol{v}_n \rangle = \langle \boldsymbol{v}_{n-1} \rangle \triangleq \langle \boldsymbol{v} \rangle$. Thus, we can get $\langle \boldsymbol{v} \rangle$ by solving Eq. (A11),

$$\langle \boldsymbol{v} \rangle = \langle \boldsymbol{L} \rangle^{-1} \cdot \langle \boldsymbol{T} \rangle \cdot \frac{\boldsymbol{F}}{m} \Delta t. \tag{A12}$$

With the help of Eqs. (A9) and (A12), the average displacement during Δt in the steady state can be derived,

$$\begin{aligned}\langle \boldsymbol{r}_n \rangle - \langle \boldsymbol{r}_{n-1} \rangle &= \langle \boldsymbol{v} \rangle \Delta t + \frac{\boldsymbol{F}}{2m} \Delta t^2 \\ &= \frac{\Delta t}{2m} \left(2 \langle \boldsymbol{L} \rangle^{-1} \cdot \langle \boldsymbol{T} \rangle + \boldsymbol{I} \right) \cdot \boldsymbol{F} \Delta t \\ &= \frac{\Delta t}{2m} \left(2 \langle \boldsymbol{L} \rangle^{-1} - \boldsymbol{I} \right) \cdot \boldsymbol{F} \Delta t. \end{aligned} \tag{A13}$$

Thus, the terminal velocity is

$$\boldsymbol{v}_f = \frac{\Delta t}{2m} \left(2 \langle \boldsymbol{L} \rangle^{-1} - \boldsymbol{I} \right) \cdot \boldsymbol{F}, \tag{A14}$$

and the mobility tensor reads

$$\boldsymbol{\mu} = \frac{\Delta t}{2m} \left(2 \langle \boldsymbol{L} \rangle^{-1} - \boldsymbol{I} \right). \tag{A15}$$

Finally, by comparing Eqs. (A8) and (A15), the Einstein relation of the CSRD fluid is explicitly proven,

$$\boldsymbol{D} = k_B T \boldsymbol{\mu}. \tag{A16}$$

REFERENCES

[1] E. Kalz, H. D. Vuijk, I. Abdoli, J.-U. Sommer, H. Löwen, and A. Sharma, Phys. Rev. Lett. **129**, 090601 (2022).

[2] P. L. Muzzeddu, H. D. Vuijk, H. Löwen, J.-U. Sommer, and A. Sharma, J. Chem. Phys. **157**, 134902 (2022).

[3] C. Hargus, J. M. Epstein, and K. K. Mandadapu, Phys. Rev. Lett. **127**, 178001 (2021).

[4] J. Korving, H. Hulsman, H. F. P. Knaap, and J. J. M. Beenakker, Phys. Lett. **21**, 5 (1966).

[5] H. F. P. Knaap and J. J. M. Beenakker, Physica **33**, 643 (1967).

[6] J. E. Avron, R. Seiler, and P. G. Zograf, Phys. Rev. Lett. **75**, 697 (1995).

[7] T. Holder, R. Queiroz, and A. Stern, Phys. Rev. Lett. **123**, 106801 (2019).

[8] D. Banerjee, A. Souslov, A. G. Abanov, and V. Vitelli, Nat. Commun. **8**, 1573 (2017).

[9] M. Han, M. Fruchart, C. Scheibner, S. Vaikuntanathan, J. J. de Pablo, and V. Vitelli, Nat. Phys. **17**, 1260 (2021).

[10] L. J. F. Hermans, P. H. Fortuin, H. F. P. Knaap, and J. J. M. Beenakker, Phys. Lett. A **25**, 81 (1967).

[11] G. W. 'T Hooft, E. Mazur, J. M. Bienfait, L. J. F. Hermans, H. F. P. Knaap, and J. J. M. Beenakker, Physica A **98**, 41 (1979).

[12] M. Fruchart, M. Han, C. Scheibner, and V. Vitelli, arXiv:2202.02037 (2022).

[13] E. Eren, M. Fruchart, and V. Vitelli, arXiv:2508.12944 (2025).

[14] R. Lier and P. Matus, arXiv:2602.21367 (2026).

[15] R. Maire, A. Petrini, U. M. B. Marconi, and L. Caprini, arXiv:2603.04273 (2026).

[16] R. Zwanzig, J. Chem. Phys. **40**, 2527 (1964).

[17] R. Zwanzig, Annu. Rev. Phys. Chem. **16**, 67 (1965).

[18] H.-M. Chun, Q. Gao, and J. M. Horowitz, Phys. Rev. Res. **3**, 043172 (2021).

[19] D. J. Evans and G. Morriss, *Statistical Mechanics of Nonequilibrium Liquids*, 2nd ed. (Cambridge University Press, 2008).

[20] C. Hargus, A. Deshpande, A. K. Omar, and K. K. Mandadapu, Phys. Rev. Lett. **134**, 097105 (2025).

[21] C. Hargus, K. Klymko, J. M. Epstein, and K. K. Mandadapu, J. Chem. Phys. **152**, 201102 (2020).

[22] C. J. O. Reichhardt and C. Reichhardt, Europhys. Lett. **137**, 66004 (2022).

[23] P. Liu, H. Zhu, Y. Zeng, G. Du, L. Ning, D. Wang, K. Chen, Y. Lu, N. Zheng, F. Ye, and M. Yang, Proc. Natl. Acad. Sci. U. S. A. **117**, 11901 (2020).

[24] Q. Yang, H. Zhu, P. Liu, R. Liu, Q. Shi, K. Chen, N. Zheng, F. Ye, and M. Yang, Phys. Rev. Lett. **126**, 198001 (2021).
[25] X. Lou, Q. Yang, Y. Ding, P. Liu, K. Chen, X. Zhou, F. Ye, R. Podgornik, and M. Yang, Proc. Natl. Acad. Sci. U. S. A. **119**, e2201279119 (2022).
[26] Y. Ding, B. Wang, Q. Yang, Z. Zhao, S. Komura, R. Seto, M. Yang, and F. Ye, Research **7**, 0356 (2024).
[27] S. Succi, *The Lattice Boltzmann Equation for Fluid Dynamics and Beyond* (Oxford University Press, 2001), ISBN: 9780198503989.
[28] A. J. C. Ladd, J. Fluid Mech. **271**, 285–309 (1994).
[29] A. J. C. Ladd, J. Fluid Mech. **271**, 311–339 (1994).
[30] P. Español and P. Warren, Europhys. Lett. **30**, 191 (1995).
[31] P. J. Hoogerbrugge and J. M. V. A. Koelman, Europhys. Lett. **19**, 155 (1992).
[32] A. Malevanets and R. Kapral, J. Chem. Phys. **110**, 8605 (1999).
[33] A. Malevanets and R. Kapral, J. Chem. Phys. **112**, 7260 (2000).
[34] J. T. Padding and A. A. Louis, Phys. Rev. E **74**, 031402 (2006).
[35] G. Gompper, T. Ihle, D. M. Kroll, and R. G. Winkler, Adv. Polym. Sci. **221**, 1 (2009).
[36] M. Ripoll, K. Mussawisade, R. G. Winkler, and G. Gompper, Europhys. Lett. **68**, 106 (2004).
[37] M. Yang and M. Ripoll, Soft Matter **9**, 4661 (2013).
[38] Y. Jiao and M. Yang, Phys. Rev. E **113**, 055102 (2026).
[39] T. Ihle and D. M. Kroll, Phys. Rev. E **67**, 066705 (2003).
[40] T. Ihle and D. M. Kroll, Phys. Rev. E **67**, 066706 (2003).
[41] T. Ihle, E. Tüzel, and D. M. Kroll, Phys. Rev. E **70**, 035701 (2004).
[42] T. Ihle, E. Tüzel, and D. M. Kroll, Phys. Rev. E **72**, 046707 (2005).
[43] T. Ihle and D. M. Kroll, Phys. Rev. E **63**, 020201 (2001).
[44] Y. Jiao and M. Yang, arXiv:2508.04420 (2025).
[45] E. Kalz, H. D. Vuijk, J.-U. Sommer, R. Metzler, and A. Sharma, Phys. Rev. Lett. **132**, 057102 (2024).
[46] A. Langer, A. Sharma, R. Metzler, and E. Kalz, Phys. Rev. Res. **6**, 043036 (2024).
[47] F. Faedi, E. Kalz, R. Metzler, and A. Sharma, New J. Phys. **28**, 063501 (2026).
[48] A. R. Poggioli and D. T. Limmer, Phys. Rev. Lett. **130**, 158201 (2023).
[49] C.-C. Huang, A. Varghese, G. Gompper, and R. G. Winkler, Phys. Rev. E **91**, 013310 (2015).